14. The suckling mouse model (*10*) was used to quantify the STa-induced diarrhea in vivo. STa (50 ng) was dissolved in 0.5 ml of isotonic PBS and injected intragastrically in 3- to 4-day-old mice. After a 2-hour incubation at 25°C, the whole intestine without stomach was carefully removed and weighed. The g/c ratio was calculated as the ratio of gut weight to remaining carcass weight. To evaluate the response to CT, we used the sealed mouse model [S. H. Richardson, J. C. Giles, K. S. Kruger, *Infect. Immun.* **43**, 482 (1984)]. Data are expressed as mean ± SEM of five mice for each treatment. $P < 0.05$ versus control.
15. Bone length was determined by x-ray analysis and by analysis of alizarin-red–stained skeletons. Data are expressed as mean ± SEM. For immunohistochemistry, knees were fixed in 95% ethanol overnight and cut in 6-μm sections. Sections were incubated for 1 hour with Abs to cGKI and cGKII (*8*). The primary Abs were visualized by using a biotinylated secondary Ab (antibody to rabbit immunoglobulin G), followed by avidin-peroxidase complex and developed with H_2O_2-3,3′-diaminobenzidintetrahydrochlorid (Vectastain, Burlinghome, CA). For in situ hybridization, specimens were fixed in 4% paraformaldehyde overnight, embedded in paraffin, and cut in 6-μm sections. In situ hybridization was performed with a cGKII cDNA probe (nucleotides 960 to 1719) (*5*). [^{3}H]Thymidine labeling of growth plates was performed as described [A. M. Reimold *et al.*, *Nature* **379**, 262 (1996)], and bone transplantation was performed as described by W. J. L. Felts [*Transplant. Bull.* **4**, 5 (1957)]. Femurs of 1-week-old donors were implanted subcutaneously into 4- to 6-week-old recipients. After 14 days, the mice were killed and the length of the femurs was determined.
16. A. Pfeifer *et al.*, data not shown.
17. A. Erlebacher, E. H. Filvaroff, S. E. Gitelman, R. Derynck, *Cell* **80**, 371 (1995); E. B. Hunziker, R. K. Schenk, L. M. Cruz-Orive, *J. Bone Jt. Surg.* **69**, 162 (1987).
18. We thank K. Kühn for his advice; M. Walter, M. Guba, and I. Blumenstein for their help in the Ussing chamber experiments; K. Doerr, S. Kamm, and S. Benkert for technical assistance; and P. Klatt for help in quantifying the total body fat of the mice. Supported by grants from the Deutsche Forschungs Gemeinschaft, Bundesministerium für Forschung und Technologie, and Fonds der Chemie. R.F. was supported by the Hermann and Lilly Schilling Stiftung.

9 July 1996; accepted 2 October 1996

Control of EGF Receptor Signaling by Clathrin-Mediated Endocytosis

Amandio V. Vieira, Christophe Lamaze, Sandra L. Schmid*

Epidermal growth factor receptor (EGFR) signaling was analyzed in mammalian cells conditionally defective for receptor-mediated endocytosis. EGF-dependent cell proliferation was enhanced in endocytosis-defective cells. However, early EGF-dependent signaling events were not uniformly up-regulated. A subset of signal transducers required the normal endocytic trafficking of EGFR for full activation. Thus, endocytic trafficking of activated EGFR plays a critical role not only in attenuating EGFR signaling but also in establishing and controlling specific signaling pathways.

Signaling by ligand-activated receptor tyrosine kinases (RTKs) such as EGFR can elicit a wide range of cell type–specific responses leading to proliferation or differentiation. EGF binding triggers dimerization and trans- or autophosphorylation of the receptor, followed by recruitment and activation of SH2 (src homology domain 2) or PTB (phosphotyrosine binding) domain–containing intracellular signal transducers (*1*). Ligand binding also triggers the recruitment of EGFR to clathrin-coated pits, followed by internalization of the EGFR-ligand complex and its delivery to lysosomes for degradation (*2*). Although activated EGFR follows the canonical endocytic pathway (*3*) during this process of "down-regulation," RTK-specific regulators affecting sorting at both early (*4*, *5*) and late (*6*, *7*) trafficking steps have been identified. Many of these regulators, for example, snx-1 (sorting nexin 1) (*6*) and phosphatidylinositol 3-kinase (PI-3-kinase) (*7*), appear to affect sorting of only a subset of RTKs. Why should RTKs have their own repertoire of intracellular trafficking regulators? One possibility is that regulation of trafficking serves to modulate RTK signaling.

To examine whether EGFR endocytosis and trafficking are important for controlling the signaling pathways and cellular responses to EGF, we examined these events in cells conditionally and specifically defective in clathrin-dependent receptor-mediated endocytosis (*8*). The conditional defect in endocytosis is imposed by the regulated expression of the $Lys^{44} \rightarrow Ala^{44}$ (K44A) mutant form of dynamin (*8*), a guanosine triphosphatase that is required for clathrin-coated vesicle formation (*9*).

Ligand-induced endocytosis of EGFR was potently inhibited in cells overexpressing K44A dynamin (K44A cells) as compared with cells overexpressing comparable amounts of wild-type dynamin (WT cells) (Fig. 1A). In contrast, endocytosis of inactivated EGFR, defined as the basal rate and measured with mAb528 [an antagonistic monoclonal antibody (mAb) to EGFR] as ligand (*10*), was not significantly affected (Fig. 1A). These data confirm the role of

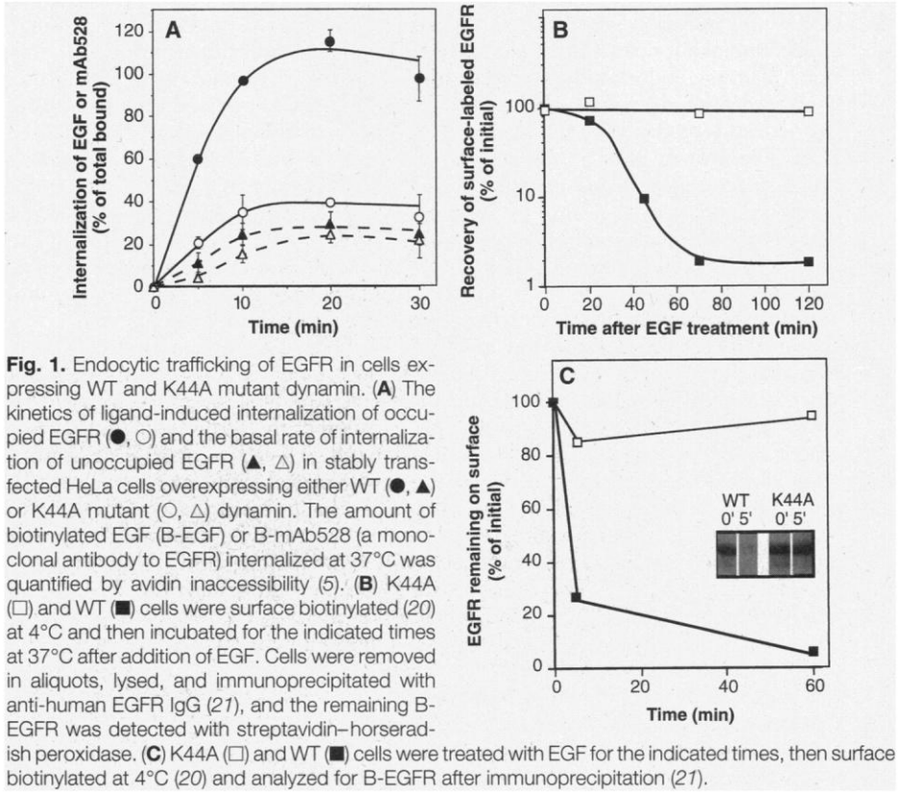

Fig. 1. Endocytic trafficking of EGFR in cells expressing WT and K44A mutant dynamin. (**A**) The kinetics of ligand-induced internalization of occupied EGFR (●, ○) and the basal rate of internalization of unoccupied EGFR (▲, △) in stably transfected HeLa cells overexpressing either WT (●, ▲) or K44A mutant (○, △) dynamin. The amount of biotinylated EGF (B-EGF) or B-mAb528 (a monoclonal antibody to EGFR) internalized at 37°C was quantified by avidin inaccessibility (*5*). (**B**) K44A (□) and WT (■) cells were surface biotinylated (*20*) at 4°C and then incubated for the indicated times at 37°C after addition of EGF. Cells were removed in aliquots, lysed, and immunoprecipitated with anti-human EGFR IgG (*21*), and the remaining B-EGFR was detected with streptavidin–horseradish peroxidase. (**C**) K44A (□) and WT (■) cells were treated with EGF for the indicated times, then surface biotinylated at 4°C (*20*) and analyzed for B-EGFR after immunoprecipitation (*21*).

Department of Cell Biology, The Scripps Research Institute, La Jolla, CA 92037, USA.

*To whom correspondence should be addressed. E-mail: slschmid@scripps.edu

clathrin-coated pits in ligand-induced EGFR endocytosis and suggest that unoccupied receptors are internalized along with the bulk plasma membrane (*11*).

Intracellular accumulation of EGF in K44A cells (Fig. 1A) reached a steady state by 10 min, which suggests that intracellular ligand-receptor complexes are either rapidly degraded or recycled. To distinguish these two possibilities, we compared EGFR down-regulation and the surface expression of EGFR in WT and K44A cells. In the absence of EGF, both WT and K44A cells expressed equal levels of the endogenous EGFR (Fig. 1, B and C). In WT cells, after a brief lag, surface EGFR was degraded with a half-time of ~30 min, whereas in K44A cells ~80% of EGFR was detected even 2 hours after EGF addition (Fig. 1B). Correspondingly, EGFR was rapidly and efficiently cleared from the surface of WT cells but not K44A cells after addition of EGF (Fig. 1C). Thus, after internalization at a basal rate, activated EGFR appeared to be efficiently recycled back to the cell surface in K44A cells, which is consistent with a previous model suggesting that endocytosis rates, not EGFR kinase activation, control EGFR down-regulation (*10*). In the absence of EGF, neither K44A nor WT cells showed any significant loss of EGFR over the 2-hour time course (*12*). Thus, in K44A cells EGFR is not subject to normal ligand-induced intracellular trafficking and degradation.

Responses to EGF were then analyzed in cells with WT or defective EGFR trafficking. First, as an endpoint of a complex series of signal transduction events, EGF-dependent proliferation of K44A and WT cells was measured after serum starvation. K44A cells showed increased EGF-dependent proliferation as assessed by either cell number–dependent catabolism of the dye MTT [(3-(4,5-dimethylthiazol-2-yl)-2,5-diphenyltetrazolium bromide] or [^{3}H]thymidine incorporation into DNA (Fig. 2, A and B). Furthermore, when K44A cells were grown in the presence of tetracycline to suppress mutant dynamin expression, they behaved indistinguishably from WT cells grown with or without induction of dynamin. Thus, overexpression of K44A dynamin, but not WT dynamin, enhanced the cell proliferative response. Because the overexpression of WT or K44A dynamin does not alter the levels of endogenous EGFR, these results establish that defective endocytic trafficking of EGFR leads to enhanced EGF-dependent proliferation, which confirms that receptor-mediated endocytosis is critical for attenuating EGFR signaling (*13*).

Early responses to EGF were examined by analyzing EGF-dependent tyrosine phosphorylation in WT and K44A cells. After serum starvation, both WT and K44A cells showed significant EGF-dependent increases in tyrosine phosphorylation, which indicates that overexpression of neither WT nor K44A dynamin led, in general, to EGF-independent activation of signaling pathways (Fig. 2C). In contrast, several proteins were either hyperphosphorylated or hypophosphorylated in K44A cells relative to WT cells after EGF stimulation (Fig. 2C). Thus, normal EGFR endocytic trafficking was required to trigger distinct signaling pathways.

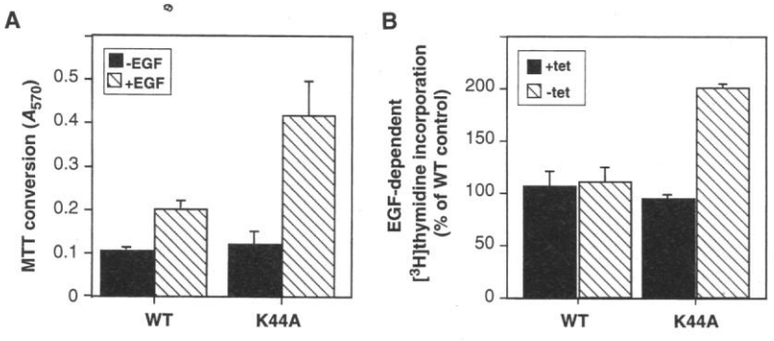

Fig. 2. EGF-dependent proliferation and tyrosine phosphorylation patterns in WT and K44A cells. (**A**) Serum-starved HeLa cells overexpressing either WT or K44A dynamin were treated with (striped bars) or without (solid bars) 4 nM EGF. After 48 hours, the enzymatic conversion of MTT was measured by absorbance at 570 nm (A_{570}) (*22*). SD (n = 3) is indicated above the bars. (**B**) K44A or WT cells were incubated in serum-free media in the presence (uninduced, solid bars) or absence (induced, shaded bars) of tetracycline (tet; 1 μg/ml). EGF-dependent incorporation of [^{3}H]thymidine into DNA was then measured (*22*) as an indication of mitogenesis. The data are shown relative to labeled DNA in cells not treated with EGF (± SD, n = 4). (**C**) HeLa cells overexpressing WT or K44A dynamin were treated (+) or not (−) with 3.5 nM EGF for 10 min. Tyrosine-phosphorylated proteins were immunoprecipitated (*21*) from whole-cell extracts with α-PY IgG (4G10) and then protein immunoblotted with the same antibody. Molecular mass standards are indicated on the left; components hyper- and hypophosphorylated in K44A relative to WT cells are indicated on the right by closed and open circles, respectively.

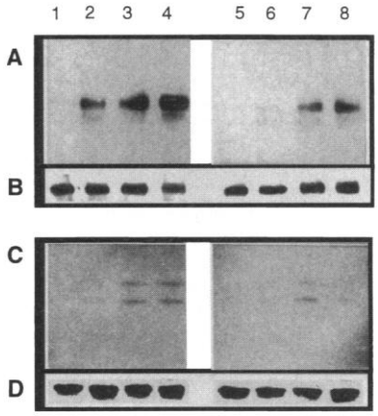

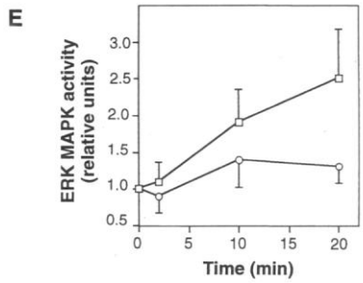

Fig. 3. EGF-dependent tyrosine phosphorylation of EGFR and MAPK (ERK1 and ERK2) is suppressed in endocytosis-defective cells. (**A** through **D**) Serum-starved K44A cells cultured in the presence (lanes 1 through 4) or absence (lanes 5 through 8) of tetracycline were treated with EGF for 0 min (lanes 1 and 5), 2 min (lanes 2 and 6), 10 min (lanes 3 and 7), or 20 min (lanes 4 and 8). Lysates prepared from equal numbers of cells were immunoprecipitated (*21*) with rabbit anti-human EGFR [(A) and (B)] or rabbit anti-rat ERK IgG [(C) and (D); upper and lower signals in (C) represent ERK1 and ERK2, respectively] and then immunoblotted with anti-phosphotyrosine [(A) and (C)], anti-EGFR (B), or anti ERK1 (D). (**E**) MAPK activity was assessed by myelin basic protein phosphorylation (*23*) with the use of anti-ERK immunoprecipitates of lysates from serum-starved WT (squares) or K44A (circles) HeLa cells that had been treated with EGF for the indicated times. [^{32}P]MBP was quantitated by densitometric scanning of autoradiographs (± SD, n = 3). MAPK activity in EGF-treated cells was expressed relative to that in untreated control cells.

To identify these pathways, the activation of known EGFR signal transducers was analyzed. EGFR was tyrosine-phosphorylated to a lesser extent in cells that overexpressed K44A dynamin (Fig. 3A) than in either WT cells (Fig. 4F) or in noninduced K44A cells (Fig. 3A). These differences were even more pronounced 20 min after addition of EGF, because EGFR degradation would have begun in WT cells (Fig. 3B). Thus, normal endocytic trafficking of activated EGFR was necessary to achieve full EGFR tyrosine phosphorylation. As is consistent with this observation, EGFR is hyperphosphorylated in endosomal versus plasma membrane fractions from rat liver (*14*). Furthermore, we have confirmed that hypophosphorylated EGFR can trigger enhanced proliferation (*15*).

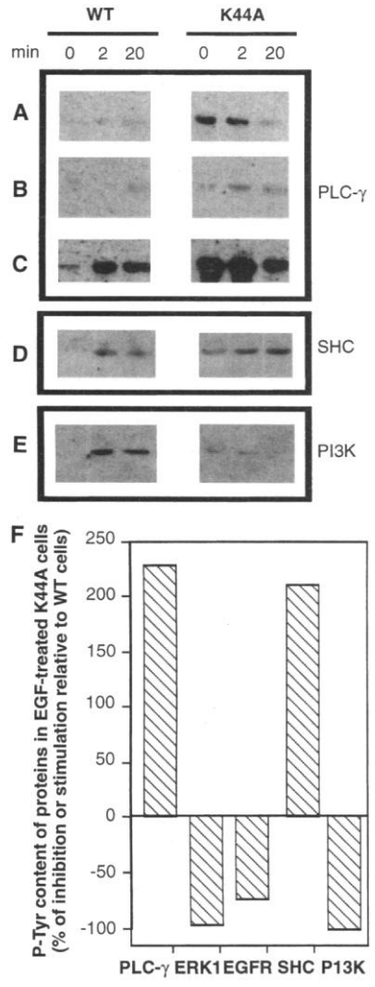

Fig. 4. Differential tyrosine phosphorylation of signal transduction components in endocytosis-defective cells. (**A** through **E**) EGF treatment of serum-starved WT or K44A cells for the indicated times was followed by immunoprecipitation of the extracts (*20*) with anti-phosphotyrosine IgG and then protein immunoblotting with mAb to bovine phospholipase Cγ–1 (PLC-γ) [(A) through (C)]; antibody to human SHC [SH2-domain containing α2 collagen-related protein; intermediate (p52/p55) form shown] (D); or antibody to rat p85 (PI3K), the 85-kD regulatory subunit of PI3K (E). The cells in (B) were cultured in the presence of tetracycline to provide an uninduced control. For comparison, in both (A) and (B) the same exposure time was used and (C) represents a longer exposure of (A). Control blots showed that the levels of SHC, PLC-γ, ERK1, and PI3K-p85 in WT and K44A cell lysates were similar (100 ± 16%) at all time points. (**F**) A quantitation of antiphosphotyrosine (anti–P-Tyr) protein immunoblot signals (20 min after EGF treatment) for the indicated signal transducers in HeLa cells overexpressing either WT or K44A dynamin. Each value represents an average of two experiments (average variation 29% for SHC, <12% for all others).

Activation of mitogen-activated protein (MAP) kinases was also suppressed in endocytosis-defective cells, as measured by both tyrosine phosphorylation of the MAP kinases ERK1 and ERK2 (Figs. 3C and 4F) and by MAP kinase activity (Fig. 3E). Thus, normal endocytic trafficking of EGFR is important for the full activation of MAP kinases (*16*).

The 85-kD regulatory subunit of PI 3-kinase (p85-PI3K) can be tyrosine-phosphorylated in response to EGF (*17*), although p85 tyrosine phosphorylation does not necessarily correlate with activation of the PI3K catalytic subunit. We found p85 to be hypophosphorylated in endocytosis-defective HeLa cells relative to WT cells in response to EGF (Fig. 4, E and F). Because PI3K activity is required for regulating receptor trafficking in endosomal compartments but not for internalization (*7*), our findings may reflect preferential activation of p85-PI3K during later events in intracelluar trafficking of EGFR. In any case, these results provide an additional example of the requirement for correct EGFR trafficking in establishing specific signaling pathways.

Among the signaling proteins that were hyperphosphorylated in endocytosis-defective cells were PLC-γ (Fig. 4, A through C and F) and SHC (Fig. 4, D and F). PLC-γ showed increased phosphorylation even in the absence of EGF, although there was not a general up-regulation of EGF-independent tyrosine phosphorylation (Fig. 2C). The significance of this finding remains to be determined. The hyperphosphorylation of PLC-γ and SHC or both (*15*) may be an important factor in the enhanced EGF-dependent hyperproliferative pathway of these cells.

Thus, in addition to initiating the clearance and down-regulation of the EGF-EGFR signaling complex, receptor trafficking plays a critical role in defining the signals transmitted by activated EGFR. Our results provide functional insight into the physiological significance of RTK-specific regulators of receptor trafficking. A comparison of the mitogenic potencies of EGF (which diverts internalized receptor-ligand complexes to late endosomes and lysosomes) and transforming growth factor–α (which dissociates from EGFR at mild acidic pH, allowing it to recycle from early endosomes) suggests that EGFR ligands have evolved to regulate their signals by controlling EGFR trafficking (*18*). Signal transducing molecules have been shown to affect membrane trafficking (*19*); here we present evidence that this regulation can flow in both directions, that is, that membrane trafficking can also regulate signal transduction events.

REFERENCES AND NOTES

1. Reviewed by P. van der Geer, T. Hunter, R. A. Lindberg, *Annu. Rev. Cell Biol.* **10**, 251 (1994); J. Schlessinger and A. Ullrich, *Neuron* **9**, 383 (1992).
2. H. T. Haigler, J. M. McKanna, S. Cohen, *J. Cell Biol.* **81**, 382 (1979).
3. A. Sorkin and C. M. Waters, *Bioessays* **15**, 375 (1993).
4. A. Sorkin and G. Carpenter, *Science* **261**, 612 (1993); A. Benmerak *et al.*, *J. Cell Biol.* **131**, 1831 (1995); Z. Wang and M. F. Moran, *Science* **272**, 1935 (1996).
5. C. Lamaze, T. Baba, T. E. Redelmeier, S. L. Schmid, *Mol. Biol. Cell* **4**, 715 (1993); C. Lamaze and S. L. Schmid, *J. Cell Biol.* **129**, 47 (1995).
6. R. C. Kurten, D. L. Cadena, G. N. Gill, *Science* **272**, 1008 (1996).
7. M. Joly, A. Kazlauskas, R. S. Fay, S. Corvera, *ibid.* **263**, 684 (1994); H. Schpetner, M. Joly, D. Hartley, S. Corvera, *J. Cell Biol.* **132**, 595 (1996).
8. H. Damke, T. Baba, D. E. Warnock, S. L. Schmid, *J. Cell Biol.* **127**, 915 (1994).
9. J.-P. Liu and P. J. Robinson, *Endocr. Rev.* **16**, 590 (1995); D. E. Warnock and S. L. Schmid, *Bioessays* **18**, 885 (1996).
10. H. S. Wiley *et al.*, *J. Biol. Chem.* **266**, 11083 (1991).
11. Endocytosis rates for bulk membrane are maintained in cells overexpressing dominant-negative mutants of dynamin by the compensatory up-regulation of clathrin-independent endocytic mechanisms [H. Damke, T. Baba, A. M. van der Bliek, S. L. Schmid, *J. Cell Biol.* **131**, 69 (1995); C. Lamaze and S. L. Schmid, *Curr. Opin. Cell Biol.* **7**, 5730 (1995)].
12. A. Vieira and S. L. Schmid, unpublished data.
13. Cells that overexpress truncated EGFR deficient in ligand-induced endocytosis exhibit increased EGF-dependent proliferation [A. Wells *et al.*, *Science* **247**, 962 (1990); H. Masui, A. Wells, C. S. Lazar, M. G. Rosenfeld, G. N. Gill, *Cancer Res.* **51**, 6170 (1991)]. In these cases, however, the proliferative response may be due to altered signaling that results from abnormal receptor structure (and overexpression, or both) and not specifically to the lack of endocytosis [S. J. Decker, C. Alexander, T. Habib, *J. Biol. Chem.* **267**, 1104 (1992)].
14. G. M. DiGuglielmo, P. C. Baass, W.-J. Ou, B. I. Posner, J. J. M. Bergeron, *EMBO J.* **13**, 4269 (1994).
15. SHC tyrosine phosphorylation is an important requirement for enhanced proliferation mediated by hypophosphorylated EGFR [N. Gotoh *et al.*, *Proc. Natl. Acad. Sci. U.S.A.* **91**, 167 (1994); N. Gotoh *et al.*, *Oncogene* **11**, 2525 (1995); R. Nishikawa *et al.*, *Proc. Natl. Acad. Sci. U.S.A.* **91**, 7727 (1994)].
16. Others have observed a lack of correlation between MAP kinase activation and enhanced proliferation [M. Holgado-Madruga, D. R. Emlet, D. K. Moscatello, A. K. Godwin, A. J. Wong, *Nature* **379**, 560 (1996); C. J. Marshall, *Cell* **80**, 179 (1995)].
17. S. P. Soltoff and L. C. Cantley, *J. Biol. Chem.* **271**, 563 (1996).
18. P. C. Baas, G. M. DiGuglielmo, F. Authier, B. I. Posner, J. J. M. Bergeron, *Trends Cell Biol.* **5**, 465 (1995).
19. P. De Camilli, S. D. Emr, P. S. McPherson, P. Novick, *Science* **271**, 1533 (1996); C. Lamaze, T.-H. Chuang, L. J. Terlecky, G. M. Bokoch, S. L. Schmid,

Nature **382**, 177 (1996).
20. Surface biotinylation was performed according to the manufacturer's instructions with the use of NHS-LC-biotin (Pierce, Rockford, IL) at 40 nmol per 10^6 cells.
21. Cell extracts (1% Triton X-100) were immunoprecipitated [4 μg of immunoglobulin G (IgG) per 400 to 600 μg of lysate per 80 μl of immobilized Protein A/G or goat antibody to mouse IgG] and subjected to protein immunoblotting (1:2000 dilution of IgG) and ECL detection. Signals were quantitated with a Molecular Dynamics system.
22. Induced K44A and WT cells were serum-starved [0.4% serum in Dulbecco's modified Eagle's medium (DMEM)] for 20 hours and then cultured for 2 days in the presence or absence of 4 nM EGF. For the last 4 hours, MTT (Sigma) was added at 1 mg/ml and its reductive conversion was measured [F. Denizot and R. Lang, *J. Immunol. Methods* **89**, 271 (1986)]. For thymidine incorporation measurements, cells (~25% confluency) in DMEM + 10% fetal bovine serum (FBS) were incubated in serum-free DMEM, with or without tetracycline (1 μg/ml), for 40 hours. EGF (3.5 nM) was then added for 18 to 20 hours. Methyl-[^{3}H]thymidine (1 μCi/ml) (Amersham) was added for the last 4 hours. Cells were then processed as described [A. Obermeier, I. Tinhofer, H. H. Grunicke, A. Ullrich, *EMBO J.* **15**, 73 (1996)], and incorporated radioactivity was quantitated in the presence of ProteinPlus scintillant (Beckman).
23. Cells were seeded at ~20% confluency in DMEM + 10% FBS without tetracycline. After 36 hours, they were incubated in DMEM without serum for 16 to 20 hours. EGF (3.5 nM) was then added for 2 to 20 min, and the cells were rinsed three times with phosphate-buffered saline and lysed with MKAL buffer [0.5% Triton X-100, 20 mM Hepes, 100 mM NaCl, 200 μM sodium orthovanadate, 10 mM NaF, 1 mM phenylmethylsulfonyl fluoride, aprotinin (1 μg/ml), leupeptin (2 μg/ml), and 1 mM dithiothreitol (pH 7.4)]. Lysate (400 μg) was immunoprecipitated with 4 μg of affinity-purified anti-ERK IgG (UBI, catalog number 06-182). To the washed immunoprecipitates was added 1/10 volume of 10× assay buffer stock [200 mM Hepes, 500 mM NaCl, 1 mM sodium orthovanadate, 200 mM $MgCl_2$, 200 μM adenosine triphosphate (ATP), and 200 mM β-glycero-phosphate (pH 7.4)]. To each tube was added 2 μCi of γ-[^{32}P]ATP and myelin basic protein (MBP; 0.25 mg/ml), and the reactants were incubated at 32°C for 15 min. [^{32}P]MBP was then quantitated as described in Fig. 3.
24. We thank G. Gill and D. Cadena for the antibodies to human EGFR and T. Hunter for critical reading of the manuscript. Supported by National Cancer Institute grants CA58689 and CA69099 to S.L.S. A.V.V. was supported by the Human Frontier of Science Programme (grant LT 461/95), and C.L. was supported by the U.S. AMRMC (grant DAM17-94-J-4031). S.L.S. is an American Heart Association Established Investigator. This is The Scripps Research Institute manuscript number 10219-CB.

20 August 1996; accepted 24 October 1996

Association of Src Tyrosine Kinase with a Human Potassium Channel Mediated by SH3 Domain

Todd C. Holmes, Debra A. Fadool, Ruibao Ren, Irwin B. Levitan*

The human Kv1.5 potassium channel (hKv1.5) contains proline-rich sequences identical to those that bind to Src homology 3 (SH3) domains. Direct association of the Src tyrosine kinase with cloned hKv1.5 and native hKv1.5 in human myocardium was observed. This interaction was mediated by the proline-rich motif of hKv1.5 and the SH3 domain of Src. Furthermore, hKv1.5 was tyrosine phosphorylated, and the channel current was suppressed, in cells coexpressing v-Src. These results provide direct biochemical evidence for a signaling complex composed of a potassium channel and a protein tyrosine kinase.

Potassium channels are important for such cellular electrical properties as resting potential, excitability, and the repolarization of the action potential. Thus, modulation of these channels can profoundly affect physiological processes including neuronal integration, vesicle secretion, and muscle contraction. The modulation of potassium channel activity by serine-threonine kinases has been studied extensively (*1*). The recently discovered PYK2 tyrosine kinase (*2*), as well as endogenous tyrosine kinases in human embryonic kidney (HEK) 293 cells (*3*), can also phosphorylate and suppress the activity of potassium channels. In spite of emerging evidence concerning the functional effects of tyrosine phosphorylation of potassium channels, there is no information available about the mechanisms of targeting and association of these channels with tyrosine kinases. However, the existence of signaling complexes consisting of ion channels and closely associated protein kinases and phosphatases has been inferred from biochemical and functional electrophysiological studies (*4*).

Specific protein-protein interactions between signaling proteins are mediated by modular binding domains (*5*). Among the first of these to be characterized was a conserved sequence found in the Src tyrosine kinase, known as the Src homology 3 (SH3) domain. SH3 domains bind to proline-rich regions in partner proteins. We examined the sequences of mammalian voltage-dependent potassium channels, and noted that several species isoforms of Kv1.5—including those from human (hKv1.5), dog, and rabbit (*6*)—contain one to two copies of the preferred Src SH3 domain binding motif RPLPXXP (*7*, *8*). In particular, hKv1.5 contains two repeats of the sequence RPLPPLP between amino acid residues 65 and 82 of the channel protein (*6*, *8*, *9*). To determine whether hKv1.5 and Src are associated in vivo, we coexpressed the channel and kinase in HEK 293 cells and tested for their interaction by immunoprecipitation followed by protein immunoblotting with specific antibodies to hKv1.5 and Src (*10*).

When hKv1.5 and associated proteins were immunoprecipitated from cell lysates with a specific antibody, Src was co-precipitated (Fig. 1A). Similarly, when Src and associated proteins were immunoprecipitated from HEK 293 cell lysates, hKv1.5 co-precipitated with endogenous and coexpressed Src (Fig. 1A). Expression of hKv1.5 protein was not altered by v-Src coexpression, as verified by protein immunoblot analysis of cell lysates with antibodies directed against tagged (Fig. 1A) and native (Fig. 2A) sequences of the channel. Furthermore, immunoblot (Fig. 1A) or protein silver stain (Fig. 3A) analysis of immunoprecipitates demonstrated that the efficiency of immunoprecipitation of hKv1.5 was not affected by v-Src coexpression. Enzymatic activity of Src also co-precipitated with hKv1.5, as detected by an in vitro kinase assay with hKv1.5 immunoprecipitates and an Src-specific substrate (*11*) (Fig. 1B).

The association between hKv1.5 and Src was also observed in human tissue. Native Src was detected in immunoprecipitates, prepared with a Kv1.5 antiserum, from human myocardium ventricle tissue lysates (Fig. 1C). The native Src that co-immunoprecipitated with native Kv1.5 co-migrated on protein immunoblots with native Src, immunoprecipitated directly with a polyclonal anti-Src antibody (Fig. 1C). Thus association of hKv1.5 and Src occurs under physiological conditions, and does not depend on expression in a heterologous system. This association may contribute to the co-localization of Kv1.5 and Src in cellular adhesion zones in myocardium (*12*). Although the stoichiometry of the association between hKv1.5 and Src is not known, only a fraction of the total myocardial Src co-immunoprecipitated with hKv1.5 (Fig. 1C), consistent with the fact that Src phosphorylates other substrates.

There are specific sequence requirements for the association of hKv1.5 and Src. For example the NH_2-terminal region of the rat Kv1.5 (rKv1.5) channel also contains a pro-

T. C. Holmes, D. A. Fadool, I. B. Levitan, Department of Biochemistry and Volen Center for Complex Systems, Brandeis University, Waltham, MA 02254, USA.
R. Ren, Department of Biology and Rosenstiel Basic Medical Sciences Research Center, Brandeis University, Waltham, MA 02254, USA.

*To whom correspondence should be addressed.